7th European Workshop on Structural Health Monitoring
July 8-11, 2014. La Cité, Nantes, France

TOPOLOGICAL IMAGING OF DEFECTS IN ANISOTROPIC PLATES

S. Rodriguez[1,3], **M. Castaings**[1], **M. Deschamps**[1], **E. Ducasse**[1,2]

[1] *Univ. Bordeaux, I2M - UMR 5295, F-33400 Talence, France*
CNRS, I2M - UMR 5295, F-33400 Talence, France
[2] *Arts et Métiers ParisTech, I2M - UMR 5295, F-33400 Talence, France*
[3] *Cooperative Research Centre for Advanced Composite Structures 1/320 Lorimer Street, Port Melbourne, Victoria, 3207, Australia*

samuel.rodriguez@u-bordeaux.fr

ABSTRACT

Topological imaging is an emerging ultrasonic imaging method based on two computations performed for the so-called reference medium. The reference medium should correspond as close as possible to the experimental medium in the absence of defects. The topological image will then highlight all the differences between the investigated experimental medium and the reference medium. The presented work aims at applying this method to the detection, location and imaging of defects in composite plates. If the propagation can be properly simulated and the associated experience performed, the defects of the medium can be imaged whatever the complexity of the propagation process. Wave propagation in composite plates is here computed considering an equivalent homogeneous anisotropic medium in the frequency regime. First a numerical experiment is presented. It consists in the investigation of a strongly anisotropic medium using two different wave modes simultaneously. Three defects are accurately located and imaged in the medium. Secondly, a real experiment is investigating an impacted quadratic composite plate is investigated with a single guided mode. Two impacts are well detected and located.

KEYWORDS : *defect detection; anisotropic plate; topological imaging; guided wave; dispersion*

1. INTRODUCTION

Ultrasounds are widely used for imaging solid media. There are numerous active techniques, all based on two principles. First, one or several transducers emit waves that propagate in the inspected media whose elastic response is measured by the same or other transducers. Then, the image is computed from the measured signals based on a more or less precise model of the wave propagation in the inspected medium. For example, the simplest model consists of assuming a constant wave velocity and associating a distance with a time of flight measurement. This is the principle used in delay and sum methods such as Bscan, SAFT [1–3], TFM [4]. The images are there defined as linear combinations of the phase-shifted measured signals. Conversely, techniques based on the time-reversal process such as DORT [5], MUSIC [6] or the time-reversal sink [7] require non-linear processing based on an eigenvector decomposition or a spatio-temporal maximum energy detection. Topological imaging [8–13] also requires non-linear processing as the two wave fields obtained numerically are multiplied together before being integrated over the frequency domain. All these techniques have already been successfully applied for inspecting solid media with bulk waves, using either transducer arrays or a single moving transducer.
Structures such as plates act as a guide for elastic waves where an infinity of modes may propagate. Two difficulties arise when imaging waveguides. First, coupling the transducers with the structure

makes it difficult to select a specific mode for the emission or the reception and multiple mode propagation is complex to deal with. Second, the dispersive nature of guided waves implies shape distortion of the wave packets. Nevertheless, these difficulties can be overcome with a fine understanding of the physical phenomena and by using adapted transducers and/or signal processing. A review of imaging approaches based on Lamb waves is given in [14]. Using classical and enhanced delay and sum algorithms, Wilcox [15] developed a plate imaging system where the plate is investigated in all directions simultaneously with an axisymmetrical distribution of transducers that excite and detect only the S_0 mode. Dispersion is taken into account with a frequency-dependent phase velocity. The Synthetic Aperture Focusing Technique was adapted to Lamb waves [2] leading to the so-called L-SAFT method. In this method, the F-SAFT algorithm [16] is applied with a frequency-dependent phase velocity and a single transducer is used for exciting and detecting the S_0 mode.

Wilcox presented a method that removes the effect of dispersion [17]. These methods result in a re-compression of the wave packet and hence an image whose resolution is comparable to that obtained with non-dispersive waves. They all rely on single mode propagation. Monomodal propagation can be achieved by filtering out individual modes from multimodal wave packets if suitable phase shifts are applied to each element of a matrix array in the frequency domain [18]. This method allows excited and detected modes to be properly selected. Experimental time-reversal was achieved with Lamb waves [19], demonstrating re-compression and self-focusing to be possible using guided waves. Synthetic time reversal imaging is thus possible [20].
So far, topological imaging has mainly been experimentally applied to fluids and solids inspected with bulk waves [8, 10–13]. Topological optimization is a mathematical method which was first applied to optimize mechanical structures; it was thus dealing with elastostatic problems. Its application to elastodynamic problems such as the investigation of materials with ultrasonic waves started in the last decade [9, 21–23]. This imaging technique has been recently applied to detect defects in isotropic plate using guided Lamb waves [24]. In the present study, this latter approach is successfully applied to anisotropic material plates.

2. TOPOLOGICAL IMAGING IN ANISOTROPIC WAVEGUIDES

Topological imaging is a recent experimental method introduced in applied mathematics for topological optimization. The application of topological optimization to elastodynamic inverse problems has been addressed for example in [21, 22]. The required mathematical developments are beyond the scope of this paper. Here we simply recall the basic principles of the imaging method resulting from the application of topological optimization by the adjoint method, the so-called topological imaging method. Skipping all calculations, the main result is that an image of the medium is obtained by plotting the topological gradient which is directly computed from the solutions of two simple propagation problems [21], [9]. This image is given by the following integral

$$G(M) = \left| \int_{\mathbb{R}^+} \widehat{u}(M,\omega).\widehat{v}(M,\omega) d\omega \right|, \tag{1}$$

where $\widehat{u}(M,\omega)$ and $\widehat{v}(M,\omega)$ are spectra of the so-called direct and adjoint field. The symbol $\widehat{\ }$ on functions indicates that the function represents a time spectrum. These two fields result from the same propagation problem, for a defect less medium, but with two different sources. In the present case, the field $\widehat{w}$ resulting from the radiation in the domain Ω of a source, located on the surface Γ, defined by $z = 0$ (see Figure 1), and expressed by the function $\hat{\mathbf{S}}$, is solution of the following system :

$$\begin{cases} \rho\omega^2\widehat{w} + \nabla.(C : \nabla\widehat{w}) = 0 \text{ in } \Omega, \\ \hat{\sigma}\,|_{x=\pm h/2} = 0, \\ \hat{\sigma}\,|_{\Gamma} = \hat{\mathbf{S}}, \end{cases} \tag{2}$$

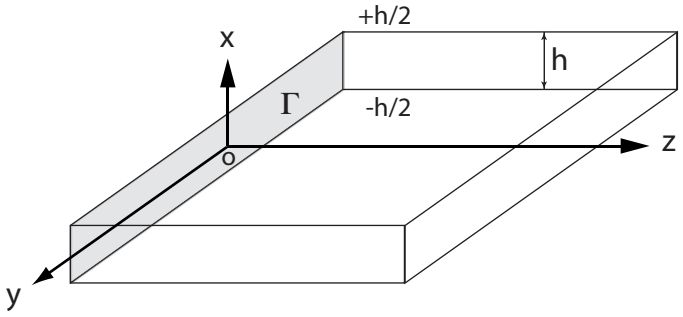

Figure 1 : Geometry of the problem.

with ρ, C, ω and h, respectively, the density, the elastic tensor, the angular frequency and the thickness of the plate and where the three equations correspond, respectively, to the propagation equation, the free boundary conditions on the two plate interfaces and the source condition. For the direct problem, $\widehat{w} = \widehat{u}(M,\omega)$ and $\hat{\mathbf{S}} = \hat{\mathbf{S}}_o$, where $\hat{\mathbf{S}}_o$ simulate the amplitude repartition created by the transducers which are located on the surface Γ. For the adjoint problem, $\widehat{w} = \widehat{v}(M,\omega)$ and $\hat{\mathbf{S}} = \hat{\mathbf{S}}_{exp}$, with $\hat{\mathbf{S}}_{exp} = \alpha(\widehat{v}_{exp} - \widehat{u}|_\Gamma)^*$, where α is a constant, the superscript * indicates complex conjugation, $\widehat{v}_{exp}$ and $\widehat{u}|_\Gamma$ represent the measured and calculated fields on the surface Γ, respectively.

The solutions of this system can be expressed by a Lamb modes summation coupled with a double Fourier integral, in terms of the wave number along the y-direction, k_y , and ω.

To illustrate the great potential of topological imaging two examples will be traited in the two next sections. First, a strongly anisotropic plate will be analyzed. Second, a significant wave dispersion will be dealt with to detect defects in a slightly anisotropic plate. In spite of these complex physical phenomena, the imaging process works as long as they are correctly taken into account in the propagation model.

3. NUMERICAL EXPERIMENT ON A UNIDIRECTIONAL FIBER COMPOSITE

In this section, the experiment is numerically simulated. The plate under consideration is a single layer of unidirectional carbon fiber composite. Within the frequency range of calculations, such a composite material can be considered as an hexagonal homogeneous medium for which the equivalent density is ρ=1560$kg \cdot m^{-3}$ and the homogenized stiffnesses are: c_{11}=14, c_{22}=86.6, c_{33}=13.5, c_{44}=4.7, c_{55}=2.72, c_{66}=4.06, c_{12}=6.40, c_{13}=6.40, c_{23}=9 [GPa]. The crystallographic directions ♯1, ♯2 and ♯3 correspond to the x-, y- and z-axis, respectively. The direction of fibers coincides with the y-axis. The plate thickness is of 3.6mm.

The anisotropic plate and the source are presented Figure 2. The source is located on the cross section defined by $z = 0$. The amplitude of the imposed force follows a narrow Gaussian distribution along the y-direction and is invariant in the x-direction. With such a source and in the frequency range of the signal, only the two fundamental modes SH_0 (horizontal shear wave) and S_0 (compressional wave) are generated with a significant amplitude. Three holes are located at the distance z=12 cm from the source.

To simulate the experiment, by using finite element methods, the calculation of the interaction between the source $\hat{\mathbf{S}}_o$ and the defects is done. Then, the field scattered by the defects is obtained at the source plane, i.e. on the surface Γ defined in eq. 2. From these calculations, the source associated to the adjoint problem $\hat{\mathbf{S}}_{exp}$ can be calculated. The direct and adjoint fields, $\widehat{u}(M,\omega)$ and $\widehat{v}(M,\omega)$, are calculated from modes expansion associated to a 2D Fourier analysis [24]. Note that the two generated modes with this source interact with the defects and they create two reflected wavefronts associated with these two modes. To expand the adjoint source $\hat{\mathbf{S}}_{exp}$ in terms of Lamb waves, it is necessary to

separate these modal contributions. This selection is done by sampling the field in the x-direction in addition to the sampling in the y-direction, which is done to obtain the space Fourier transformation in terms of k_y. The image is then calculated for $x = 0$ by the expression given by Eq. 1. Clearly, the three defects are identified on the obtained image, as shown in Figure 3.

In the study presented in [24], it has been shown the great interest of the topological method to image defects in isotropic plates even when the guided wave propagation is strongly dispersive. In the present study, the efficiency of this method, based on field calculations, is emphasized for large anisotropy. Indeed, the anisotropic behavior of the wave propagation is very strong for such long fiber composites. To examine this point, Figure 4 shows, in polar coordinates and for the central frequency of 100 kHz, the phase and group velocities of the two guided waves that propagated in the plate plane. The complexity of the group velocity of SH_0 mode in such material is made clear. This is visible on the SH_0 wavefront which exhibits a cusp. This means that for some specific directions, i.e. for some specific transducers for a given defect, the SH_0 mode can produce three contributions on the waveform, as has been shown experimentally on this plate [25]. It is of great interest to note that even with this strong anisotropy, i.e. with cusp existence, no artefact is seen in the image.

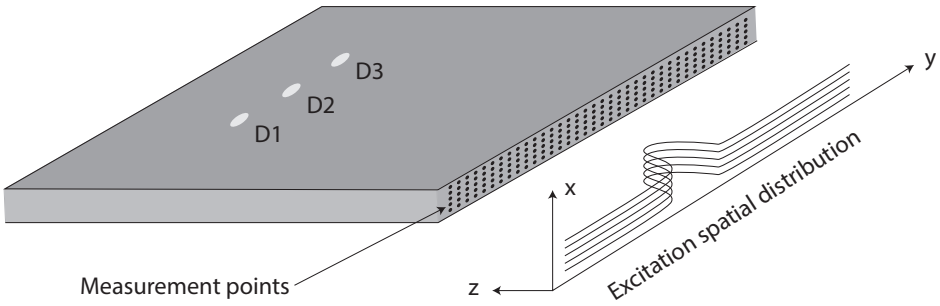

Figure 2 : Numerical configuration - Plate, defects, measurement points and source.

4. EXPERIMENT ON A LAMINATE COMPOSITE

In this section, one real experiment is presented to image a laminate composite plate made of 16 plies with orientations of 0, 90, 45 and - 45 degrees. The mechanical properties of the associated homogeneous material are : ρ=1520$kg \cdot m^{-3}$, c_{11}=15, c_{22}=56.0, c_{33}=56.0, c_{44}=16.5, c_{55}=2.5, c_{66}=2.5, c_{12}=10.2, c_{13}=10.2, c_{23}=23.0 [GPa]. The plate thickness is of 2.25mm.

The experiments consist of firing all the elements of a linear array simultaneously and recording the scattered field on each channel individually. The array is coupled to the plate along its edge so that the transducers produce and are sensitive to the in-plane motion (Figure 5). The array is composed of 128 transducers whose central frequency is 500 kHz and which are assumed to be identical. The response is measured over the 150-350 kHz frequency range. The pitch of the array is $l = 2.5$ mm. Thus the whole array is 32 cm long. The transducers are 10 mm high. In the investigated plate of 2.25mm thick, the transducers then cover the whole thickness of the plate. The transducer width e is 2 mm. In the experiments, wavelengths are no shorter than 5 mm. Thus, even in the extreme case where a wave propagates parallel to the array, the spatial sampling satisfies the Nyqvist criterion. Thus emitted and recorded signals can be considered as continuous function versus y without any aliasing. Signals are emitted and sampled with a Lecoeur OPEN multi-channel system set to 10 MHz sampling frequency. Plate insonification consists of emitting the same wave simultaneously from all transducers. As a result, the source $\hat{\mathbf{S}}_o$ applied along the z-axis at the plane $z = 0$ is quasi-plane. The signal used is a three-cycle Hamming-Windowed sinusoidal signal with central frequency equal to 200 KHz. Such a signal covers the whole frequency bandwidth of the transducers. Using wide frequency content provides as much information on the medium as possible with a given device.

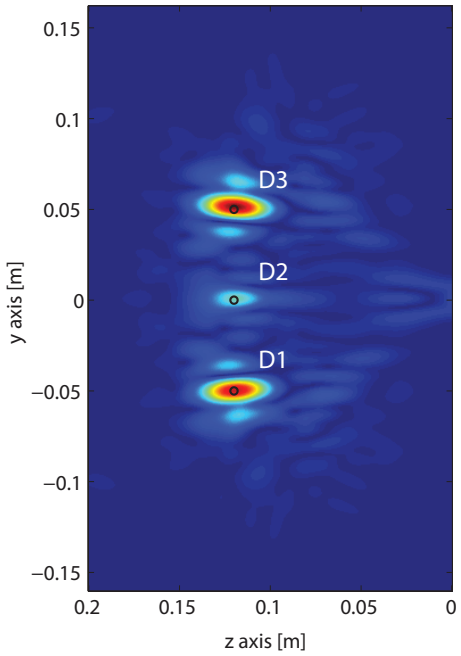

Figure 3 : Topological image for a monolayer plate of carbon epoxy.

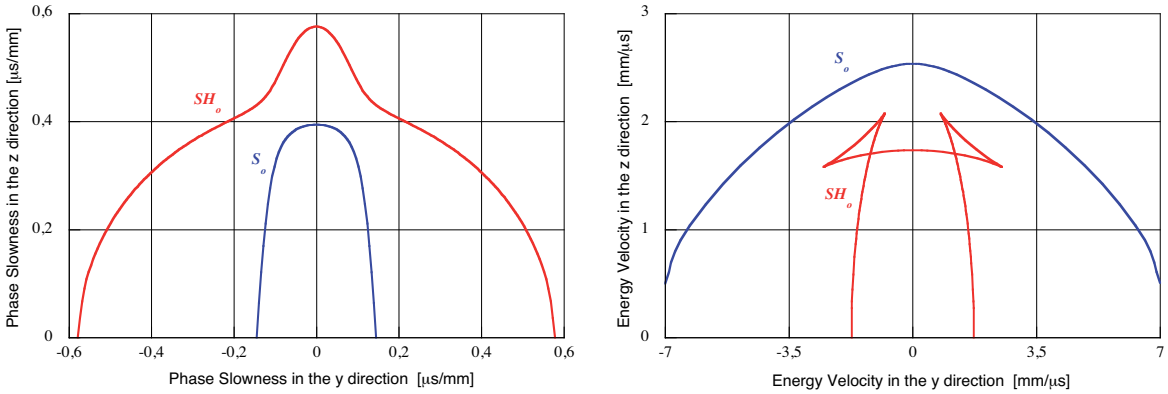

Figure 4 : Phase velocity (a) and group velocity (b) of the SH_0 and S_0 modes at the frequency of 100 kHz.

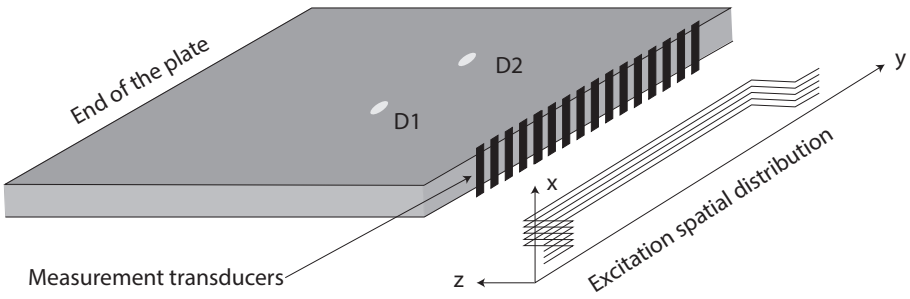

Figure 5 : Experiment configuration - Plate, defects, measurement points and sources.

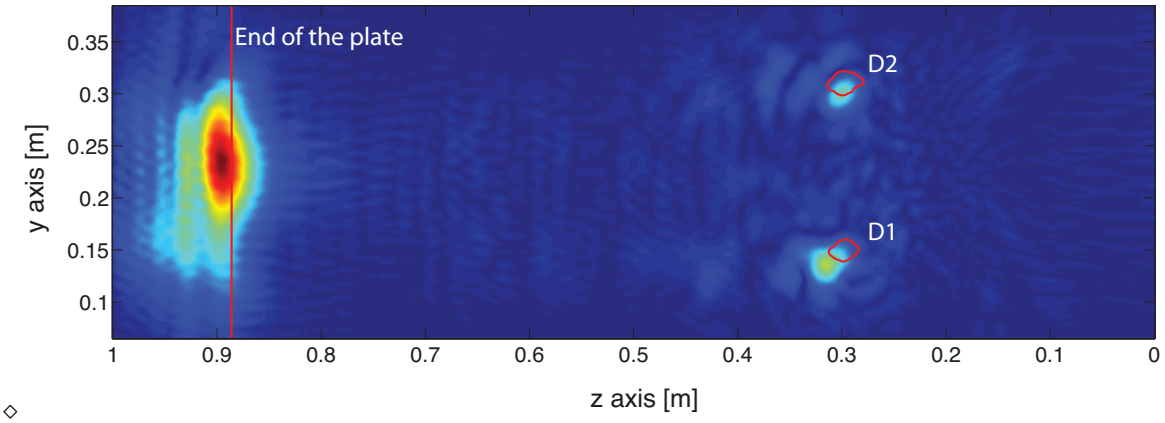

Figure 6 : Topological image for a laminate composite plate $[0/90/45,\text{-}45]_{2S}$, with two impact dammages D_1 and D_2, using S_0 mode at 150-350 kHz. Red circle lines indicate measurement data obtained from a classical water-immesion C-Scan technique with focussed transducers.

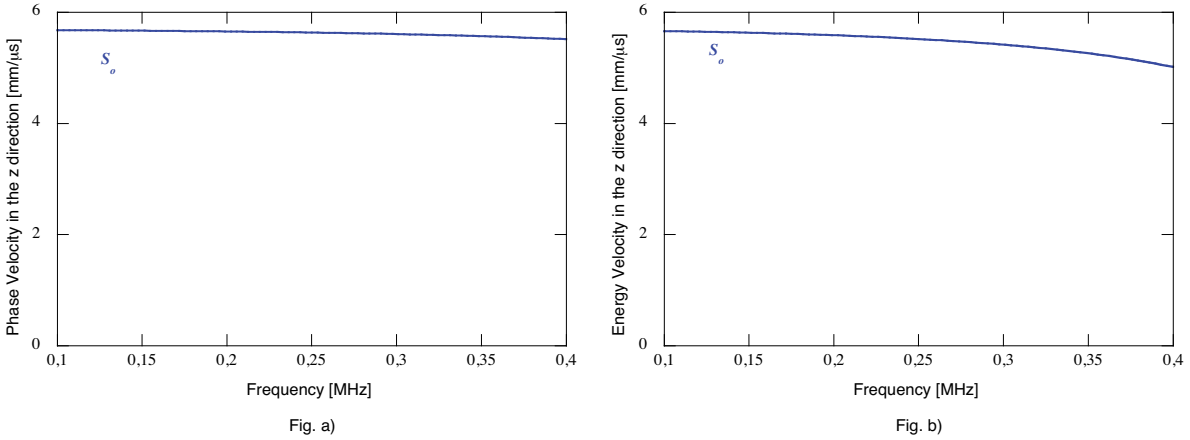

Figure 7 : Dispersion curves of the phase velocity (a) and the group velocity (b) of the S_0 mode for a propagation in the z-direction.

Referring to Eq. 1, computing the topological image requires the solutions of direct and adjoint problems for a chosen value of x. In contrast with the numerical experiments described in section 3, the acoustic field cannot be sampled in the x-direction. The main consequence is that only one mode can be dealt with, since it is not possible to separate different Lamb wave contributions. From an experimental point of view, the source $\hat{\mathbf{S}}_o$ generates only the S_0 mode in the frequency range of inspection. To satisfy the monomodal analysis, it is then assumed that not any mode conversions occur from diffraction by defects. The defects created on the plate results from two impacts. The symmetry is then broken. Consequently, the assumption of monomodal conversion is not necessarely true. This point will require further investigations. All the same, let us assume the validity of the monomodal approximation. Then, the fields associated to both direct and adjoint problems are calculated. The obtained image is shown in Figure 6.

Let us analyse now the image. The positions of defects, characterized by a C-Scan experiment, have been ploted on the topological image of Figure 6. They are identified by the red forms. The position of the end of the plate is as well identified by the red line. First, note the correct detection and localization of both defects by the topological image. In addition, the end of the plate is also localised on the image. This is because the reflection on this edge is not modelled in the reference medium

and consequently it appears as a defect. Second, let us analyse the wave propagation. The plane of propagation is quasi-isotropic, but the S_0 mode is slightly dispersive in the experimental frequency range. This is illustrated in Figure 7, where the phase and the group velocities of this mode, that propagates following the z-axis, are plotted versus the frequency. The dispersion is not very strong, but it is large enough to expand the time response of waves propagating over such long distances, i.e. about 2 m long path of propagation for the wave reflected by the end of the plate. Clearly, this dispersion does not affect the image, as it was already mensionned for an aluminum plate [24].

The time needed by the method to build the image depends on the performance of the propagation model of the reference medium. Here, a semi-analytical model based on Fourier analysis is used so that the image of a one-meter long and half-meter wide composite structure is computed in about 10 seconds.

5. CONCLUSIONS

Applying the topological imaging to the inspection by Lamb waves of anisotropic plates allows a fast and accurate inspection of these plates, as well as the construction of 2D images representing the plane of the plate. With a single ultrasonic insonification of the medium and after a few seconds of computation, impact dammages are detected and located in composite plates. In contrast to classical and advanced delay and sum methods, topological imaging implies separate processing of the signals emitted and those measured. For instance, it does not involve explicit computations of rays between emitters, potential defects and receivers. This necessary information is implicitly taken into account in the two wave field computations performed for the defect-free medium. Consequently, if wave propagation can be accurately simulated in a given medium then potentially this medium can be imaged. As an illustration, it has been demonstrated in this paper that topological imaging could handle very strong anisotropy without the image being affected. The proposed method presents a strong potential for detecting and imaging damages in SHM configurations.

ACKNOWLEDGEMENTS

This work was undertaken within the Systems Development for Structural Health Monitoring project, part of a CRC-ACS (Cooperative Research Centre for Advanced Composite Structures) research program, established and supported under the Australian Government's Cooperative Research Centers Program. The experimental set-up was funded by the *Conseil Régional d'Aquitaine*. The authors would like to thank Catherine Froustey and Nicolas Guillaud (I2M - DuMas Dpt.) for providing the impacted composite plate and Anissa Meziane (I2M - APy Dpt. and *Institut de Maintenance Aéronautique*) for letting us use their C-Scan system.

REFERENCES

[1] L.J. Busse. Three-dimensional imaging using a frequency-domain synthetic aperture focusing technique. *IEEE Trans. Ultrason. Ferroelec. Freq. Contr.*, 39:174–179, 1992.

[2] R. Sicard, J. Goyette, and D. Zellouf. A saft algorithm for Lamb wave imaging of isotropic plate-like structures. *Ultrasonics*, 39:487–494, 2002.

[3] M. Spies and W. Jager. Synthetic aperture focusing for defect reconstruction in anisotropic media. *Ultrasonics*, 41:125–131, 2003.

[4] B. W. Drinkwater C. Holmes and P. D. Wilcox. Post-processing of the full matrix of ultrasonic transmit-receive array data for non-destructive evaluation. *NDT&E Int*, 38:701–711, 2005.

[5] E Kerbrat, C Prada, D Cassereau, and M Fink. Imaging in the presence of grain noise using the decomposition of the time reversal operator. *J. Acoust. Soc. Am.*, 113:1230–1240, 2003.

[6] A.J. Devaney. Time reversal imaging of obscured targets from multistatic data. *Antennas and Propagation, IEEE Transactions on*, 53(5):1600–1610, 2005.

[7] Eric Bavu and Alain Berry. Super-resolution imaging of sound sources in free field using a numerical time-reversal sink. *Acta Acustica u. with Acustica*, 95:595–604, 2009.

[8] N. Dominguez and V. Gibiat. Non-destructive imaging using the time domain topological energy method. *Ultrasonics*, 50:367–372, 2010.

[9] N. Dominguez, V. Gibiat, and Y. Esquerre. Time domain topological gradient and time reversal analogy: an inverse method for ultrasonic target detection. *Wave Motion*, 42:31–52, 2004.

[10] V Gibiat, P Sahuguet, and A Chouippe. Wave guide imaging through time domain topological energy. *Physics Procedia*, 3:523–531, 2010.

[11] P. Sahuguet, A. Chouippe, and V. Gibiat. Biological tissues imaging with time domain topological energy. *Physica Procedia*, 3:677–683, 2010.

[12] S. Rodriguez, P. Sahuguet, V. Gibiat, and X. Jacob. Fast topological imaging. *Ultrasonics*, 52:1010–1018, 2012.

[13] S. Rodriguez, X. Jacob, and V. Gibiat. Plane wave echo particle image velocimetry. In *Proceedings of Meetings on Acoustics*, volume 19, 2013.

[14] L. Zeng and J. Lin. Structural damage imaging approaches based on Lamb waves: A review. In *International Conference on Quality, Reliability, Risk, Maintenance, and Safety Engineering (ICQR2MSE)*, 2011.

[15] P.D. Wilcox. Omni-directional guided wave transducer arrays for the rapid inspection of large areas of plate structures. *IEEE Trans. Ultrason., Ferroelect., Freq. Contr.*, 50:699–709, 2003.

[16] A. Blouin, D. Lévesque, C. Néron, D. Drolet, and J.-P. Monchalin. Improved resolution and signal-to-noise ratio in laser-ultrasonics by saft processing. *Optics Express*, 1998.

[17] P Wilcox, M Lowe, and P Cawley. The effect of dispersion on long-range inspection using ultrasonic guided waves. *NDT&E International*, 34(1):1–9, 2001.

[18] A. Leleux, P. Micheau, and M.Castaings. Long range detection of defects in composite plates using Lamb waves generated and detected by ultrasonic phased array probes. *J Nondestruct Eval*, 32(2):200–214, 2013.

[19] R.K. Ing and M. Fink. Time-reversed Lamb waves. *IEEE Trans. Ultrason., Ferroelect.,Freq. Contr.*, 45:1032–1043, 1998.

[20] C. H. Wang, J. T. Rose, and F.-K. Chang. A synthetic time-reversal imaging method for structural health monitoring. *Institute of Physics publishing - Smart materials and structures*, 13:415–423, 2004.

[21] M. Bonnet and B. Guzina. Sounding of finite solid bodies by way of topological derivative. *International Journal for numerical methods in engineering*, 61:2344–2373, 2004.

[22] M. Bonnet. Topological sensitivity of energy cost functional for wave-based defect identification. *C.R. Mécanique*, 338:377–389, 2010.

[23] S. Amstutz and N. Dominguez. Topological sensitivity analysis in the context of ultrasonic non-destructive testing. *Engineering Analysis with Boundary Elements*, 32:936–947, 2013.

[24] Rodriguez S., Deschamps M., Castaings M., and Ducasse E. Guided wave topological imaging of isotropic plates. *Ultrasonics*, In press:http://dx.doi.org/10.1016/j.ultras.2013.10.001, 2014.

[25] Guillaume Neau. *Lamb waves in anisotropic viscoelastic plates: study of the wave fronts and attenuation*. PhD thesis, Bordeaux I University, 2003.